AD NUMBER
AD328775
CLASSIFICATION CHANGES
TO: unclassified
FROM: confidential
LIMITATION CHANGES
TO: Approved for public release, distribution unlimited
FROM: Distribution authorized to U.S. Gov't. agencies and their contractors; Administrative/Operational Use; 11 Aug 1961. Other requests shall be referred to Naval Ordnance Lab., White Oak, MD.
AUTHORITY
31 Aug 1973, Group-4, DoDD 5200.10; USNOL ltr, 29 Aug 1974

AD 328 775

BALLISTICS RANGE FIRINGS FOR DETERMINATION OF DRAG AND STABILITY OF MODELS OF FIVE POLARIS CONFIGURATIONS (U)

NOL

11 AUGUST 1961

UNITED STATES NAVAL ORDNANCE LABORATORY, WHITE OAK, MARYLAND

Ballistics Research Report 42

BALLISTICS RANGE FIRINGS FOR DETERMINATION OF DRAG AND STABILITY OF MODELS OF FIVE POLARIS CONFIGURATIONS

Prepared by:

Zigurds J. Levensteins

ABSTRACT: Drag and stability characteristics of models of five POLARIS re-entry body configurations were determined. The variable parameter for these configurations was the bluntness ratio of the nose. The investigation was conducted at Mach numbers between two and six. The boundary layer flow over the surface of the models was turbulent. It was found that the slope of the normal force coefficient is smaller the blunter the nose of the model. A maximum in static stability of the models was observed between Mach numbers two and three. The dynamic stability coefficients were found to be stabilizing.

U. S. NAVAL ORDNANCE LABORATORY
WHITE OAK, MARYLAND

NOLTR 61-35 11 August 1961

This report presents results determined by free-flight model firings in the NOL Pressurized Ballistics Range No. 3 and by standard ballistics range data reduction techniques.

The work reported herein was requested by Lockheed Missiles and Space Division for support in POLARIS Fleet Ballistic Missile development. The work was sponsored by the re-entry body section of the Special Projects Office, Bureau of Naval Weapons, under task assignment NOL-335.

The author expresses gratitude to Mr. John J. Brady for enlightening comments and discussions on the subject of data reduction techniques, to Miss Amy A. Chamberlin for efficient reduction of the data and to members of the Ballistic Design and Operations Division operating the ballistics ranges for suggestions in designing the models and their sabots and for efficient execution of the model launchings.

W. D. COLEMAN
Captain, USN
Commander

A. E. SEIGEL
By direction

CONTENTS

ILLUSTRATIONS

Tables

SYMBOLS

d	diameter of the cylindrical body of the model (d = 1 caliber)
r	radius of the cylindrical body of the model
L	overall length of the model
ℓ	length of the ellipsoidal nose of the model
ℓ/r	bluntness ratio of the nose of the model
X_{CG}	distance from the center of gravity to the tip of the nose of the model
S	cross-sectional area of the cylindrical body of the model = $\frac{\pi d^2}{4}$
m	mass of the model
I	transverse moment of inertia of the model
M	reference Mach number, or aeroballistic moment acting on model
V	reference velocity of the model
ρ	air density in the range
Re_d	Reynolds number based on body diameter
α	complex angle of attack, $\alpha_H + i\alpha_V$
$\dot{\alpha}$	time rate of change of angle of attack
q	transverse angular velocity of the model
δ^2	mean squared yaw $\delta^2 \equiv \frac{1}{n}\sum^{n} \alpha_n^2$ where n is the number of measurements made
C_D	drag coefficient = $\frac{\text{drag force}}{\frac{1}{2}\rho V^2 S}$

SYMBOLS

$C_{N\alpha}$ slope of normal force coefficient = $\frac{\text{normal force}}{\alpha \, \frac{1}{2} \rho V^2 S}$

$C_{M\alpha}$ slope of static moment coefficient = $\frac{M_\alpha \alpha}{\alpha \, \frac{1}{2} \rho V^2 S d}$

X_{CP} distance between tip of nose of the model and point of application of normal force = $\frac{C_{M\alpha}}{C_{N\alpha}} + X_{c.g.}$

$C_{M_q} + C_{M_{\dot\alpha}}$ dynamic stability coefficient =

$$= \frac{M_q q}{\frac{qd}{V} \frac{1}{2} \rho V^2 S d} + \frac{M_{\dot\alpha} \dot\alpha}{\frac{\dot\alpha d}{V} \frac{1}{2} \rho V^2 S d}$$

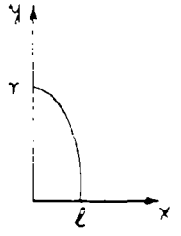

$(x/\ell)^{2.5} + (y/r)^2 = 1$, nose contour of N_1,

bluntness ratio $\ell/r = 0.5$

M_α slope of static moment with respect to angle of attack

$M_{\dot\alpha}$ slope of damping moment with respect to time rate of change of angle of attack

M_q slope of damping moment with respect to transverse angular velocity of model

BALLISTICS RANGE FIRINGS FOR DETERMINATION OF DRAG AND STABILITY OF MODELS OF FIVE POLARIS CONFIGURATIONS

INTRODUCTION

1. In order to aid in developing the aerodynamic characteristics of the re-entry body of the POLARIS Fleet Ballistic Missile, the Lockheed Missiles and Space Division requested the NOL Ballistics Department to perform a series of firings in its ballistics ranges with models of possible POLARIS re-entry body configurations. It was requested that from these firings drag, and static and dynamic stability characteristics of the models be determined at Mach numbers two, four, and six, and at such Reynolds numbers that would make the boundary layer flow over the surface of the models turbulent.

MODEL AND TEST DESCRIPTION

2. The general re-entry body configuration proposed for this investigation was a body of revolution made up of an ellipsoidal nose, cylindrical body, and frustum of a cone skirt. The parameter to be varied was the bluntness ratio of the nose, ℓ/r, the ratio of the semi-minor and semi-major axis of the ellipsoid. The designation of the various sections making up the re-entry body was adopted from LMSD and was as follows: N for the nose section, B for the body section, and S for the skirt section, all with numerical subscripts for distinguisning particular configurations. The body and skirt configuration used in the entire investigation was B_1S_3 which was joined to five noses: N_1, N_5, N_{10}, N_3, and N_4 of bluntness ratios 0.5, 0.2, 0.4, 0.6, and 0.8, respectively. The nose configuration N_1 was an exception in that it was not exactly ellipsoidal, but its contour followed the equation $(x/\ell)^{1.5} + (y/r)^2 = 1$. Also, at the time the N_1 had been designated the design nose, and for that reason more investigation was performed with it than with the other nose configurations. Measured from the tip of the nose each NBS configuration had a different reference center of gravity location, $X_{CG\ Ref.}$. The five configurations of re-entry body models used in this investigation are illustrated in Figure 1.

3. The designing and manufacturing of the models for proper center of gravity location and for sufficient structural strength to withstand the launching acceleration loads were performed by the Naval Ordnance Laboratory. One-inch body diameter models

were used for the M = 2 firings, while for the higher velocity launchings at M = 4 and 6 a 0.5 inch body diameter model was used. The 0.5 inch body diameter models for all five configurations are illustrated in Figure 2. In Table I are listed the measured quantities of the pertinent physical characteristics of all models fired.

4. All model firings for this investigation were performed in the Pressurized Ballistics Range No. 3. A general view of the range is shown in Figure 3. The main reason for choosing this range was the capability of adjusting the air pressure in it, thus forming the proper medium for meeting the Reynolds number requirements. The range and its capabilities are described in detail in reference (a). All model launchings were made from a high velocity 40-mm powder gun.

AERODYNAMIC COEFFICIENTS

5. The information obtained from these firings was reduced to the form of usable aerodynamic coefficients by the usual ballistics range data reduction technique. Both magnitude and direction of the aerodynamic forces and moments acting on the model were inferred from measuring the location of the center of gravity and angular orientation of the model at a number of observation stations along the range. In Figure 4 representative plots of the yawing motions of models are illustrated. Each numbered point on the continuous trace represents an observation station. The basic characteristics of all of these motions are the same. The markedly different appearance of the traces, representing the flight history of the angular orientations of the models, is due to different magnitudes of the starting values of the angular orientation and rate of change of the angular orientation. These quantities were not controlled in the test firings. The ballistics range data reduction technique is described in detail in reference (b).

6. The numerical results obtained by methods described in paragraph 5 are tabulated in Table II.

Drag Coefficient

7. The drag coefficients (C_D as a function of Mach number) are presented in Figure 5. The coefficients are based on the cross-sectional area of the cylindrical body. As mentioned previously in paragraph 2, the configuration $N_1B_1S_3$ was investigated more extensively than the other four. For completeness, some drag coefficients for $N_1B_1S_3$ obtained from another testing program in NOL ballistics ranges at transonic velocities were included in the graph.

8. Inspection of results revealed that the drag coefficients do not depend on the angle of attack* in the range of Mach numbers and angles of attack investigated (mean squared yaw δ^2 up to about 140 degrees squared). This conclusion was also drawn in reference (c) where information from several experimental sources has been compiled.

9. The effect of the nose bluntness ratio ℓ/r on the drag coefficient is shown in Figure 6. For the bluntness ratios investigated this relationship appears to be almost linear.

Slope of Normal Force Coefficient

10. Where it was possible the slopes of the normal force coefficients were corrected for angle of attack effect by assuming a linear relationship between this parameter (C_{N_α}) and the mean squared yaw δ^2. The slopes of the normal force coefficient corrected to zero yaw $C_{N_{\alpha_o}}$ as a function of Mach number are plotted in Figure 7. A rather great scatter in the results can be observed, especially around Mach number 2.

11. By plotting the slopes of the normal force coefficient versus the bluntness ratio of the nose, it was found that the slope of the normal force coefficient is smaller the blunter the nose of the model. This is illustrated in Figure 8. Furthermore, the relationship, for the bluntness ratios and Mach numbers covered in this investigation, is nearly linear.

Slope of Static Moment Coefficient

12. By employing the slopes of normal force coefficient C_{N_α} determined in this investigation, the magnitudes of the slopes of static moment coefficient C_{M_α} were adjusted to the specified reference center of gravity locations. Because the slopes of the normal force coefficient were generally less accurately determined than the slopes of the static moment coefficient, the accuracy of the latter also decreased.

13. The effect of angle of attack on the slopes of the static moment coefficient wherever possible was removed by assuming a linear relationship between C_{M_α} and δ^2.

---

*In ballistics range practice, the square of the angle of attack is assumed to be represented by δ^2 - the mean squared yaw. For complete appraisal of the conditions, however, it should only be considered in conjunction with the plots of the yawing motions of the models described in paragraph 5.

14. The graphs in Figure 9 illustrate the dependency of the slopes of static moment coefficient on the Mach number. The dashed portions of the curves were drawn by utilizing information from reference (c) and by assuming that, since the essential characteristics of all five configurations were the same, the general form of the curves should also be the same. Inspection of these results shows that models of all five re-entry body configurations in this investigation were statically stable, however, a decrease in static stability occurred around Mach number 2.

Center of Pressure of Normal Force

15. The center of pressure of the normal force was determined by dividing the slope of the static moment coefficient C_{M_α} by the slope of the normal force coefficient C_{N_α}. Since the magnitude of C_{N_α} increased monotonically with decreasing Mach numbers, as can be seen in Figure 7, it was concluded that the decrease in static stability around M = 2 must have been due to a movement of the location of the center of pressure of the normal force closer to the center of gravity. In Figure 10 the center of pressure X_{CP} is plotted as a function of Mach number. Also, the location of the reference center of gravity $X_{CG\ ref.}$ is indicated. From this the decrease of the static margin or moment arm of the static moment (X_{CP} - $X_{CG\ ref.}$) can be seen.

16. For drawing the dashed portions of the graphs in Figure 10, results from reference (c) were utilized.

Dynamic Stability Coefficient

17. At the Mach numbers and angles of attack in this investigation it was found that the dynamic stability coefficients $C_{M_q} + C_{M_{\dot\alpha}}$ had a stabilizing influence on the motion of the re-entry body models. That the oscillatory motions of the models were damping, or that they were dynamically stable, could be seen from the yawing motion plots. Representative plots of the yawing motions are shown in Figure 4. Because the prototype and model moments of inertia were not properly scaled, this information applies directly only to the models.

18. The scatter in the dynamic stability coefficients as a function of Mach number for all five configurations was found to be great. Consequently, no individual curves for each configuration are plotted, but only a band is indicated within which fall the dynamic stability coefficients of all five configurations. This is illustrated in Figure 11.

19. Usually the dynamic stability coefficients are defined by

$$C_{M_q} + C_{M_{\dot{\alpha}}} = \frac{M_q q}{\frac{qd}{2V}\ \frac{1}{2}\rho V^2 S d} + \frac{M_{\dot{\alpha}}\dot{\alpha}}{\frac{\dot{\alpha}d}{2V}\ \frac{1}{2}\rho V^2 S d}$$

Attention is drawn to the fact that in keeping with the practice of LMSD the coefficients in this investigation differ from the above in that they are non-dimensionalized by the divisors $\frac{\dot{\alpha}d}{V}$ and $\frac{qd}{V}$. The magnitudes here reported are thus half as large as those non-dimensionalized in the usual way as shown above.

CONCLUSIONS

20. From results determined by these ballistics range model firings and standard range data reduction techniques, the following conclusions may be drawn: between Mach numbers two and six and with turbulent boundary layer flow over the surface of the models the drag coefficients do not depend on angle of attack up to δ^2 of about 140 degrees^2; the slope of the normal force coefficient increases as the bluntness ratio of the nose increases; the static stability of the models decreases around Mach number 2 which is due to a forward movement of the center of pressure of the normal force, the dynamic stability coefficients have a stabilizing influence on the dynamic stability of the models.

REFERENCES

(a) May, A. and Williams, T.J., "Free-Flight Ranges at the Naval Ordnance Laboratory," NavOrd Report 4063, 1955

(b) Murphy, C.H., "Data Reduction for the Free-Flight Spark Ranges," BRL Report No. 900, 1954

(c) Karchmar, L., "Mark I Re-Entry Body Aerodynamic Design Data," LMSD Report 4463, 1958 (C)

TABLE I

PHYSICAL SIZE AND PROPERTIES OF MODELS

Configuration	Round Number	d (In.)	L (In.)	m (Gm.)	I ($Gm.in.^2$)	$X_{C.G.}$ (Cal.)
$N_1B_1S_3$	2760	0.998	3.111	192.74	171.3	1.343
	2761	0.999	3.110	191.63	166.9	1.331
	2762	0.999	3.109	192.94	169.6	1.329
	2751	0.999	3.111	192.74	169.27	1.330
	2687	1.000	3.105	193.58	171.47	1.340
	2688	0.999	3.111	193.88	171.64	1.341
	2753	1.000	3.111	193.74	171.63	1.340
	2681	0.499	1.547	24.88	4.83	1.259
	2694	0.999	3.107	192.69	169.72	1.336
	2695	0.999	3.111	191.98	169.29	1.336
	2745	0.499	1.550	24.94	4.92	1.263
	2724	0.500	1.547	25.00	4.92	1.256
	2834	0.500	1.555	25.19	4.91	1.256
	2728	0.499	1.555	31.34	7.30	1.515
	2729	0.499	1.549	31.15	7.27	1.511
	2730	0.500	1.555	31.25	7.32	1.512
	2732	0.500	1.552	31.34	7.22	1.502
	2731	0.499	1.555	31.35	7.17	1.515
	2826	0.501	1.552	31.35	7.31	1.500
	2692	0.999	3.110	190.97	166.96	1.329
	2690	0.999	3.110	192.25	169.11	1.334
	2764	0.999	3.109	192.84	168.94	1.336
	2763	1.000	3.109	192.99	169.55	1.334

TABLE I

PHYSICAL SIZE AND PROPERTIES OF MODELS

Configuration	Round Number	d (In.)	L (In.)	m (Gm.)	I (Gm.in.^{2})	$X_{C.G.}$ (Cal.)
$N_1B_1S_3$	2683	0.499	1.547	24.93	4.87	1.259
	2696	1.000	3.110	193.27	171.45	1.338
	2697	0.999	3.110	192.84	168.69	1.330
	2698	1.000	3.111	193.16	171.00	1.338
$N_5B_1S_3$	2756	0.500	1.477	22.83	4.03	1.136
	2757	0.500	1.475	22.80	4.02	1.136
	2863	0.998	2.958	184.71	129.42	1.201
	2864	0.999	2.958	184.74	129.41	1.202
	2722	0.500	1.477	22.81	4.03	1.132
	2723	0.499	1.477	22.78	4.01	1.140
	2765	0.499	1.476	22.78	4.03	1.146
	2725	0.499	1.476	22.83	4.03	1.134
	2727	0.500	1.477	22.87	4.04	1.132
	2842	0.499	1.480	22.84	4.06	1.138
$N_{10}B_1S_3$	2855	1.000	3.058	194.65	147.01	1.280
	2865	0.999	3.061	194.37	146.80	1.281
	2854	0.999	3.059	194.21	146.49	1.279
	2837	0.500	1.529	24.29	4.52	1.220
	2838	0.500	1.528	24.37	4.54	1.218
	2839	0.500	1.529	24.13	4.54	1.218
	2758	0.499	1.527	24.15	4.56	1.226
	2705	0.500	1.529	24.19	4.56	1.226
	2836	0.500	1.530	24.25	4.52	1.220

TABLE I

PHYSICAL SIZE AND PROPERTIES OF MODELS

Configuration	Round Number	d (In.)	L (In.)	m (Gm.)	I ($Gm.in.^2$)	$X_{C.G.}$ (Cal.)
$N_{10}B_1S_3$	2737	0.500	1.530	30.55	6.82	1.462
	2876	0.500	1.529	30.36	6.70	1.462
	2877	0.500	1.529	30.43	6.80	1.464
	2744	0.498	1.532	30.26	6.66	1.468
	2874	0.501	1.518	30.16	6.59	1.457
	2875	0.500	1.529	30.30	6.74	1.462
$N_3B_1S_3$	2847	0.499	1.580	25.75	5.36	1.329
	2713	0.500	1.577	25.72	5.39	1.324
	2848	0.499	1.581	25.77	5.38	1.331
	2709	0.500	1.577	25.62	5.37	1.336
	2710	0.499	1.579	25.73	5.41	1.329
	2708	0.500	1.574	25.65	5.33	1.324
$N_4B_1S_3$	2850	0.999	3.259	217.35	194.36	1.473
	2754	0.500	1.629	27.22	6.16	1.422
	2718	0.499	1.631	26.97	6.15	1.431
	2717	0.499	1.628	27.12	6.14	1.417
	2719	0.500	1.629	26.98	6.14	1.428

TABLE II

DRAG AND STABILITY COEFFICIENTS OF MODELS

CONFIGURATION	$N_1B_1S_3$			
Round Number	2760	2761	2762	2751
M	0.97	0.99	0.80	1.85
$Re_d \times 10^{-6}$	0.26	0.26	0.12	3.09
P.E. yaw (deg.)	0.32	0.98	0.19	0.54
P. E. swerve (in.)	0.009	0.011	0.008	0.022
δ^2 (deg.^{2})	8.8	19.4	2.8	3.7
C_D	1.536	1.838	1.132	1.846
P.E. C_D	0.003	0.009	0.005	0.001
$C_{N\alpha}$ /deg.	-0.160	-0.152	-0.124	-0.0500
P.E. $C_{N\alpha}$	0.015	0.011	0.043	0.007
$C_{N\alpha_o}$				
$C_{M\alpha}$ /deg.	-0.2030	-0.1535	-0.2640	-0.0103
P.E. $C_{M\alpha}$	0.0016	0.0040	0.0033	0.0007
$C_{M\alpha}$ ref.	-0.2170	-0.1660	-0.2735	-0.0143
$C_{M\alpha_o}$ ref.				
$X_{C.P._o}$ (cal.)	2.600	2.350	3.450	1.532
$C_{M_q} + C_{M_{\dot{\alpha}}}$/rad.	10.9	51.9	87.1	-9.7
P.E. $C_{M_q} + C_{M_{\dot{\alpha}}}$	5.9	17.2	14.2	4.8

TABLE II

DRAG AND STABILITY COEFFICIENTS OF MODELS

CONFIGURATION	$N_1B_1S_3$			
Round Number	2687	2688	2753	2681
M	2.10	2.15	2.20	3.65
$Re_d \times 10^{-6}$	3.52	3.75	3.73	2.00
P.E. yaw (deg.)	0.19	0.38	0.11	0.38
P.E. swerve (in.)	0.011	0.018	0.013	0.029
δ^2 (deg.^{2})	0.5	1.5	3.8	5.2
C_D	1.821	1.774	1.766	1.601
P.E. C_D	0.001	0.001	0.001	0.002
$C_{N\alpha}$ /deg.	-0.0513	-0.0510	-0.0525	-0.0415
P.E. $C_{N\alpha}$	0.004	0.004	0.002	0.008
$C_{N\alpha}{}_o$				
$C_{M\alpha}$ /deg.	-0.0105	-0.0138	-0.0164	-0.0131
P.E. $C_{M\alpha}$	0.0007	0.0005	0.0002	0.0002
$C_{M\alpha}$ ref.	-0.0152	-0.0183	-0.0211	-0.0134
$C_{M\alpha}{}_o$ ref.				-0.0130
$X_{C.P.}{}_o$ (cal.)	1.545	1.605	1.655	1.580
$C_{M_q} + C_{M_{\dot\alpha}}$/rad.	-12.1	-14.0	-9.1	-7.5
P.E. $C_{M_q} + C_{M_{\dot\alpha}}$	3.9	2.8	0.5	1.2

TABLE II

DRAG AND STABILITY COEFFICIENTS OF MODELS

CONFIGURATION	$N_1B_1S_3$			
Round Number	2694	2695	2745	2724
M	3.79	3.80	5.92	5.97
$Re_d \times 10^{-6}$	4.19	4.30	1.68	1.69
P.E. yaw (deg.)	0.18	0.17	1.19	1.04
P.E. swerve (in.)	0.013	0.029	0.011	0.014
δ^2 (deg.^{2})	3.4	11.5	135.8	102.8
C_D	1.516	1.530	1.506	1.467
P.E. C_D	0.002	0.001	0.001	0.004
$C_{N\alpha}$ /deg.	-0.0433	-0.0381	-0.0419	-0.0379
P.E. $C_{N\alpha}$	0.002	0.002	0.002	0.001
$C_{N\alpha_o}$			-0.0304	-0.0290
$C_{M\alpha}$ /deg.	-0.0120	-0.0131	-0.0269	-0.0197
P. E. $C_{M\alpha}$	0.0002	0.0002	0.0003	0.0002
$C_{M\alpha}$ ref.	-0.0157	-0.0164	-0.0274	-0.0202
$C_{M\alpha_o}$ ref.	-0.0154	-0.0150	-0.0090	-0.0080
$X_{C.P.}$ (cal.)	1.630	1.678	1.545	1.525
$C_{M_q} + C_{M_{\dot{\alpha}}}$/rad.	-7.5	-7.7	-4.2	-2.2
P.E. $C_{M_q} + C_{M_{\dot{\alpha}}}$	1.2	0.6	1.7	2.0

TABLE II

DRAG AND STABILITY COEFFICIENTS OF MODELS

CONFIGURATION	$N_1B_1S_3$			
Round Number	2834	2728	2729	2730
M	6.01	3.86	4.12	4.18
$Re_d \times 10^{-6}$	1.68	2.23	2.32	2.30
P.E. yaw (deg.)	0.40	0.64	0.40	0.36
P.E. swerve (in.)	0.014	0.016	0.024	0.015
δ^2 (deg.^{2})	61.9	11.0	22.5	18.5
C_D	1.465	1.503	1.521	1.502
P.E. C_D	0.001	0.002	0.002	0.001
C_{N_α} /deg.	-0.0340	-0.0389	-0.0398	-0.0365
P.E. C_{N_α}	0.002	0.0009	0.0009	0.0007
$C_{N_{\alpha_o}}$	-0.0291	-0.0380	-0.0380	-0.0350
C_{M_α} /deg.	-0.0117	-0.0027	-0.0040	-0.0030
P.E. C_{M_α}	0.0002	0.0002	0.0002	0.0002
C_{M_α} ref.	-0.0119	-0.0130	-0.0143	-0.0123
$C_{M_{\alpha_o}}$ ref.	-0.0088	-0.0120	-0.0118	-0.0108
$X_{C.P.}$ (cal.)	1.551	1.565	1.560	1.558
$C_{M_q}+C_{M_{\dot\alpha}}$ /rad.	-5.2	-4.0	-6.3	-7.5
P.E. $C_{M_q} + C_{M_{\dot\alpha}}$	0.8	2.2	0.9	0.8

TABLE II

DRAG AND STABILITY COEFFICIENTS OF MODELS

CONFIGURATION	$N_1B_1S_3$			
Round Number	2732	2731	2826	2692
M	5.78	5.83	5.89	2.24
$Re_d \times 10^{-6}$	1.62	1.63	2.03	2.11
P.E. yaw (deg.)	0.91	0.77	0.88	0.20
P.E. swerve (in.)	0.014	0.015	0.014	0.016
δ^2 (deg.^{2})	44.2	79.9	88.1	4.6
C_D	1.444	1.457	1.453	1.720
P.E. C_D	0.003	0.002	0.002	0.001
$C_{N\alpha}$ /deg.	-0.0332	-0.0366	-0.0381	-0.0539
P.E. $C_{N\alpha}$	0.0005	0.001	0.0009	0.003
$C_{N\alpha_o}$	-0.0300	-0.0296	-0.0310	
$C_{M\alpha}$ /deg.	-0.0028	-0.0063	-0.0068	-0.0157
P.E. $C_{M\alpha}$	0.0002	0.0002	0.0002	0.0002
$C_{M\alpha}$ ref.	-0.0111	-0.0159	-0.0165	-0.0199
$C_{M\alpha_o}$ ref.	-0.0092	-0.0088	-0.0076	-0.0194
$X_{C.P.}$ (cal.)	1.556	1.546	1.494	1.620
$C_{M_q} + C_{M_{\dot{\alpha}}}$ /rad.	-4.9	-3.7	-2.0	-4.9
P.E. $C_{M_q} + C_{M_{\dot{\alpha}}}$	2.2	2.7	1.8	1.3

TABLE II

DRAG AND STABILITY COEFFICIENTS OF MODELS

CONFIGURATION	$N_1B_1S_3$			
Round Number	2690	2764	2763	2683
M	2.26	2.26	2.28	3.69
$Re_d \times 10^{-6}$	2.08	2.17	2.18	1.05
P.E. yaw (deg.)	0.18	0.15	0.12	0.56
P.E. swerve (in.)	0.015	0.012	0.015	0.022
δ^2 (deg.^{2})	0.5	4.1	0.6	49.8
C_D	1.702	1.711	1.696	1.594
P.E. C_D	0.001	0.002	0.002	0.001
C_{N_α} /deg.	-0.0501	-0.0558	-0.0454	-0.0386
P.E. C_{N_α}	0.007	0.003	0.008	0.003
$C_{N_\alpha}{}_o$				-0.0345
C_{M_α} /deg.	-0.0154	-0.0162	-0.0155	-0.0206
P.E. C_{M_α}	0.0005	0.0002	0.0003	0.0002
C_{M_α} ref.	-0.0195	-0.0208	-0.0194	-0.0209
$C_{M_{\alpha_o}}$ ref.		-0.0200		-0.0155
$X_{C.P.}{}^o$(cal.)	1.638	1.620	1.678	1.698
$C_{M_q} + C_{M_{\dot\alpha}}$/rad.	-8.5	-9.6	-14.0	-5.0
P.E. $C_{M_q} + C_{M_{\dot\alpha}}$	3.5	1.4	2.8	.8

TABLE II

DRAG AND STABILITY COEFFICIENTS OF MODELS

CONFIGURATION	$N_1B_1S_3$			$N_5B_1S_3$
Round Number	2696	2697	2698	2756
M	4.14	4.22	4.36	1.78
$Re_d \times 10^{-6}$	2.35	2.40	2.48	0.51
P.E. yaw (deg.)	0.14	0.10	0.22	0.20
P.E. swerve (in.)	0.014	0.011	0.013	0.014
δ^2 (deg.^{2})	11.0	3.8	49.3	0.9
C_D	1.492	1.487	1.479	2.024
P.E. C_D	0.004	0.004	0.004	0.001
$C_{N\alpha}$ /deg.	-0.0374	-0.0398	-0.0419	-0.048
P.E. $C_{N\alpha}$	0.001	0.002	0.0007	0.014
$C_{N\alpha}{}_o$	-0.0365	-0.0392	-0.0376	
$C_{M\alpha}$ /deg.	-0.0110	-0.0096	-0.0157	-0.0159
P.E. $C_{M\alpha}$	0.0002	0.0002	0.0002	0.0003
$C_{M\alpha}{}_{ref.}$	-0.0143	-0.0123	-0.0194	-0.0176
$C_{M\alpha_o}{}_{ref.}$	-0.0132	-0.0124	-0.0143	
$X_{C.P.}$ (cal.)	1.611	1.565	1.629	1.469
$C_{M_q} + C_{M_{\dot{\alpha}}}$/rad.	-6.2	-5.7	-5.2	-16.1
P.E. $C_{M_q} + C_{M_{\dot{\alpha}}}$	1.2	1.4	.8	2.2

TABLE II

DRAG AND STABILITY COEFFICIENTS OF MODELS

CONFIGURATION	$N_5B_1S_3$			
Round Number	2757	2863	2864	2722
M	1.78	1.98	1.98	3.48
$Re_d \times 10^{-6}$	0.51	3.35	3.38	1.96
P.E. yaw (deg.)	0.78	0.32	0.37	0.37
P.E. swerve (in.)	0.020	0.015	0.012	0.012
δ^2 (deg.^{2})	21.0	0.5	2.0	1.4
C_D	2.019	2.007	2.026	1.737
P.E. C_D	0.002	0.001	0.001	0.003
$C_{N\alpha}$/deg.	-0.057	-0.062	-0.054	-0.033
P.E. $C_{N\alpha}$	0.004	0.012	0.004	0.006
$C_{N\alpha_o}$				-0.0327
$C_{M\alpha}$/deg.	-0.0166	-0.0134	-0.0164	-0.0126
P.E. $C_{M\alpha}$	0.0003	0.0010	0.0005	0.0003
$C_{M\alpha}$ ref.	-0.0188	-0.0195	-0.0218	-0.0136
$C_{M\alpha_o}$ ref.				-0.0135
$X_{C.P.}$(cal.)	1.430	1.414	1.500	1.512
$C_{M_q} + C_{M_{\dot{\alpha}}}$/rad.	-9.4	-12.2	-8.8	-8.6
P.E. $C_{M_q} + C_{M_{\dot{\alpha}}}$	2.7	4.9	2.1	2.2

TABLE II

DRAG AND STABILITY COEFFICIENTS OF MODELS

CONFIGURATION	$N_5B_1S_3$			
Round Number	2723	2765	2725	2727
M	3.60	3.61	5.60	5.63
$Re_d \times 10^{-6}$	2.01	2.08	1.58	1.59
P.E. yaw (deg.)	0.40	0.72	0.77	0.34
P.E. swerve (in.)	0.013	0.009	0.012	0.015
δ^2 (deg.^{2})	2.4	8.0	66.2	7.0
C_D	1.756	1.776	1.682	1.657
P.E. C_D	0.002	0.003	0.003	0.004
$C_{N\alpha}$/deg.	-0.038	-0.037	-0.028	-0.024
P.E. $C_{N\alpha}$	0.006	0.003	0.001	0.002
$C_{N\alpha_o}$	-0.0377	-0.0362	-0.0227	-0.0233
$C_{M\alpha}$/deg.	-0.0127	-0.0126	-0.0155	-0.0058
P.E. $C_{M\alpha}$	0.0002	0.0003	0.0002	0.0002
$C_{M\alpha}$ ref.	-0.0141	-0.0143	-0.0166	-0.0064
$C_{M\alpha_o}$ ref.	-0.0140	-0.0135	-0.0058	-0.0052
$X_{C.P.}$(cal.)	1.470	1.472	1.355	1.322
$C_{M_q} + C_{M_{\dot{\alpha}}}$/rad.	-6.4	-6.6	-4.4	-6.8
P.E. $C_{M_q} + C_{M_{\dot{\alpha}}}$	1.5	1.8	1.1	1.8

TABLE II

DRAG AND STABILITY COEFFICIENTS OF MODELS

CONFIGURATION	$N_5B_1S_3$	$N_{10}B_1S_3$		
Round Number	2842	2855	2865	2854
M	5.82	1.92	2.00	2.01
$Re_d \times 10^{-6}$	1.61	3.28	3.34	3.39
P.E. yaw (deg.)	0.31	1.16	0.29	0.37
P.E. swerve (in.)	0.014	0.035	0.019	0.020
δ^2 (deg.^{2})	39.6	37.5	1.3	1.6
C_D	1.678	1.895	1.864	1.861
P.E. C_D	0.001	0.002	0.001	0.002
$C_{N\alpha}$/deg.	-0.027	-0.0719	-0.0539	-0.0490
P.E. $C_{N\alpha}$	0.001	0.0077	0.0066	0.0094
$C_{N\alpha_o}$	-0.0240			
$C_{M\alpha}$/deg.	-0.0099	-0.0222	-0.0136	-0.0127
P.E. $C_{M\alpha}$	0.0002	0.0009	0.0003	0.0007
$C_{M\alpha}$ ref.	-0.0110	-0.0281	-0.0180	-0.0166
$C_{M\alpha_o}$ ref.	-0.0045	-0.0174	-0.0175	-0.0162
$X_{C.P.}$(cal.)	1.287	1.590	1.529	1.540
$C_{M_q} + C_{M_{\dot\alpha}}$/rad.	-4.8	-12.5	-11.7	-10.4
P.E. $C_{M_q} + C_{M_{\dot\alpha}}$	0.6	3.6	2.2	3.7

TABLE II

DRAG AND STABILITY COEFFICIENTS OF MODELS

CONFIGURATION	$N_{10}B_1S_3$			
Round Number	2837	2838	2839	2758
M	3.42	3.86	3.99	5.60
$Re_d \times 10^{-6}$	1.99	2.18	2.24	1.60
P.E. yaw (deg.)	1.13	0.86	1.20	1.36
P.E. swerve (in.)	0.014	0.013	0.013	0.013
δ^2 (deg.^{2})	58.7	53.8	70.2	107.4
C_D	1.681	1.638	1.615	1.543
P.E. C_D	0.002	0.002	0.001	0.002
$C_{N\alpha}$/deg.	-0.0450	-0.0428	-0.0442	-0.0401
P.E. $C_{N\alpha}$	0.0023	0.0021	0.0021	0.0019
$C_{N\alpha}{}_o$	-0.0392	-0.0372	-0.0370	-0.0275
$C_{M\alpha}$/deg.	-0.0244	-0.0197	-0.0223	-0.0239
P.E. $C_{M\alpha}$	0.0003	0.0002	0.0003	0.0003
$C_{M\alpha}$ ref.	-0.0255	-0.0206	-0.0232	-0.0250
$C_{M\alpha}{}_{ref.}$	-0.0193	-0.0148	-0.0158	-0.0112
$X_{C.P.}{}^o$ (cal.)	1.691	1.597	1.626	1.606
$C_{M_q} + C_{M_{\dot\alpha}}$/rad.	-7.0	-5.8	-5.3	-6.0
P.E. $C_{M_q} + C_{M_{\dot\alpha}}$	1.6	1.1	1.5	2.1

TABLE II

DRAG AND STABILITY COEFFICIENTS OF MODELS

CONFIGURATION	$N_{10}B_1S_3$			
Round Number	2705	2836	2737	2876
M	5.70	5.92	3.67	3.67
$Re_d \times 10^{-6}$	1.61	1.65	2.16	2.17
P.E. yaw (deg.)	0.29	0.36	0.60	0.45
P.E. swerve (in.)	0.20	0.011	0.025	0.016
δ^2 (deg.^{2})	4.3	53.8	17.3	15.3
C_D	1.425	1.486	1.580	1.608
P.E. C_D		0.001	0.002	0.002
C_{N_α} /deg.	-0.0298	-0.0320	-0.0372	-0.0393
P.E. C_{N_α}	0.0037	0.0010	0.0016	0.0016
$C_{N_\alpha}{}_o$	-0.0293	-0.0280	-0.0355	-0.0378
C_{M_α} /deg.	-0.0054	-0.0113	-0.0045	-0.0047
P.E. C_{M_α}	0.0002	0.0002	0.0002	0.0002
C_{M_α} ref.	-0.0061	-0.0120	-0.0143	-0.0150
$C_{M_\alpha}{}_o$ ref.	-0.0060	-0.0094	-0.0125	-0.0132
$X_{C.P.}$ (cal.)	1.404	1.535	1.551	1.548
$C_{M_q} + C_{M_{\dot\alpha}}$/rad.	-3.2	-4.0	-6.0	-6.3
P.E. $C_{M_q} + C_{M_{\dot\alpha}}$	1.7	0.6	1.2	1.2

TABLE II

DRAG AND STABILITY COEFFICIENTS OF MODELS

CONFIGURATION	$N_{10}B_1S_3$			
Round Number	2877	2744	2874	2875
M	3.80	5.61	5.92	5.93
$Re_d \times 10^{-6}$	2.23	1.59	1.69	1.69
P.E. yaw (deg.)	0.47	0.58	0.85	0.81
P.E. swerve (in.)	0.012	0.010	0.012	0.010
δ^2 (deg.^{2})	39.4	61.9	60.1	52.8
C_D	1.608	1.534	1.492	1.507
P.E. C_D	0.002	0.003	0.001	0.001
C_{N_α}/deg.	-0.0399	-0.0321	-0.0321	-0.0328
P.E. C_{N_α}	0.0007	0.0005	0.0005	0.0003
$C_{N_\alpha}{}_o$	-0.0358	-0.0275	-0.0275	-0.0288
C_{M_α}/deg.	-0.0073	-0.0058	-0.0044	-0.0040
P.E. C_{M_α}	0.0002	0.0002	0.0002	0.0002
C_{M_α} ref.	-0.0179	-0.0144	-0.0126	-0.0126
$C_{M_\alpha}{}_o$ ref.	-0.0135	-0.0110	-0.0095	-0.0101
$X_{C.P.}$ (cal.)	1.576	1.599	1.544	1.550
$C_{M_q} + C_{M_{\dot\alpha}}$/rad.	-4.6	-2.7	-2.7	-2.9
P.E. $C_{M_q} + C_{M_{\dot\alpha}}$	0.6	1.9	1.9	1.5

TABLE II

DRAG AND STABILITY COEFFICIENTS OF MODELS

CONFIGURATION	$N_3B_1S_3$			
Round Number	2847	2713	2848	2709
M	3.91	3.64	4.12	5.71
$Re_d \times 10^{-6}$	2.23	2.11	2.34	1.63
P.E. yaw (deg.)	0.50	0.36	0.38	0.29
P.E. swerve (in.)	0.010	0.014	0.010	0.020
δ^2 (deg.^{2})	13.7	7.4	5.7	13.2
C_D	1.433	1.410	1.411	1.298
P.E. C_D	0.001	0.001	0.001	0.002
$C_{N\alpha}$ /deg.	-0.0408	-0.0471	-0.0368	-0.0339
P.E. $C_{N\alpha}$	0.002	0.005	0.003	0.002
$C_{N\alpha}{}_o$	-0.0393	-0.0464	-0.0360	-0.0326
$C_{M\alpha}$ /deg.	-0.0109	-0.0115	-0.0092	-0.0054
P.E. $C_{M\alpha}$	0.0002	0.0002	0.0002	0.0002
$C_{M\alpha}$ ref.	-0.0119	-0.0127	-0.0101	-0.0066
$C_{M\alpha}{}_o$ ref.	-0.0104	-0.0118	-0.0096	-0.0058
$X_{C.P.}$ (cal.)	1.564	1.553	1.566	1.477
$C_{M_q} + C_{M_{\dot{\alpha}}}$ /rad.	-7.2	-7.3	-10.8	-16.0
P.E. $C_{M_q} + C_{M_{\dot{\alpha}}}$	1.2	1.4	1.6	1.4

TABLE II

DRAG AND STABILITY COEFFICIENTS OF MODELS

CONFIGURATION	$N_3B_1S_3$		$N_4B_1S_3$	
Round Number	2710	2708	2850	2754
M	5.75	6.07	2.03	2.83
$Re_d \times 10^{-6}$	1.63	1.73	3.49	1.59
P.E. yaw (deg.)	0.44	0.28	0.25	0.19
P.E. swerve (in.)	0.019	0.017	0.010	0.017
δ^2 (deg.^{2})	14.2	13.5	2.4	2.3
C_D	1.318	1.304	1.613	1.442
P.E. C_D	0.002	0.003	0.001	0.001
C_{N_α} /deg.	-0.0325	-0.0323	-0.060	-0.050
P.E. C_{N_α}	0.002	0.009	0.002	0.007
$C_{N_{\alpha_o}}$	-0.0315	-0.0313		
C_{M_α} /deg.	-0.0056	-0.0044	-0.0068	-0.0124
P.E. C_{M_α}	0.0002	0.0002	0.0002	0.0002
C_{M_α} ref.	-0.0063	-0.0052	-0.0110	-0.0136
$C_{M_{\alpha_o}}$ ref.	-0.0055	-0.0046		
$X_{C.P.}$ (cal.)	1.474	1.446	1.590	1.666
$C_{M_q} + C_{M_{\dot\alpha}}$ /rad.	-8.0	-6.2	-10.8	-11.6
P.E. $C_{M_q} + C_{M_{\dot\alpha}}$	1.7	1.1	1.9	1.7

TABLE II

DRAG AND STABILITY COEFFICIENTS OF MODELS

CONFIGURATION	$N_4B_1S_3$		
Round Number	2718	2717	2719
M	5.72	5.81	6.12
$Re_d \times 10^{-6}$	1.64	1.66	1.75
P.E. yaw (deg.)	0.23	0.25	0.47
P.E. swerve (in.)	0.012	0.013	0.016
δ^2 (deg.^{2})	26.1	5.6	56.0
C_D	1.205	1.229	1.203
P.E. C_D	0.002	0.002	0.004
C_{N_α} /deg.	-0.0373	-0.034	-0.0391
P.E. C_{N_α}	0.0005	0.001	0.0007
$C_{N_\alpha}{}_o$	-0.0345	-0.0335	-0.0335
C_{M_α} /deg.	-0.0054	-0.0024	-0.0094
P.E. C_{M_α}	0.0002	0.0002	0.0002
C_{M_α} ref.	-0.0064	-0.0030	-0.0105
$C_{M_{\alpha_o}}$ ref.	-0.0026	-0.0024	-0.0030
$X_{C.P.}$ (cal.)	1.474	1.471	1.489
$C_{M_q} + C_{M_{\dot{\alpha}}}$ /rad.	-4.2	-3.3	-4.1
P.E. $C_{M_q} + C_{M_{\dot{\alpha}}}$	0.6	1.6	1.0

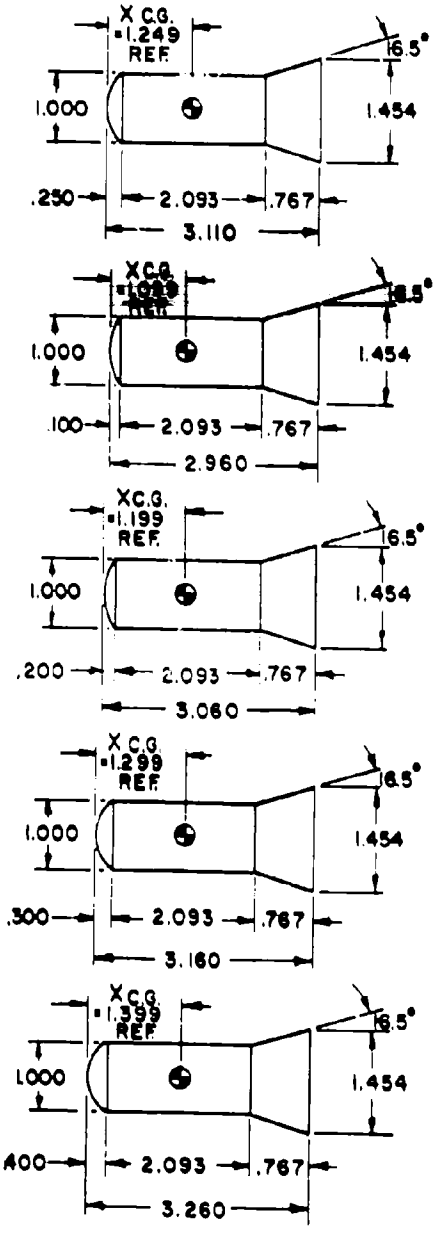

FIG. 1 CONFIGURATIONS OF MODELS

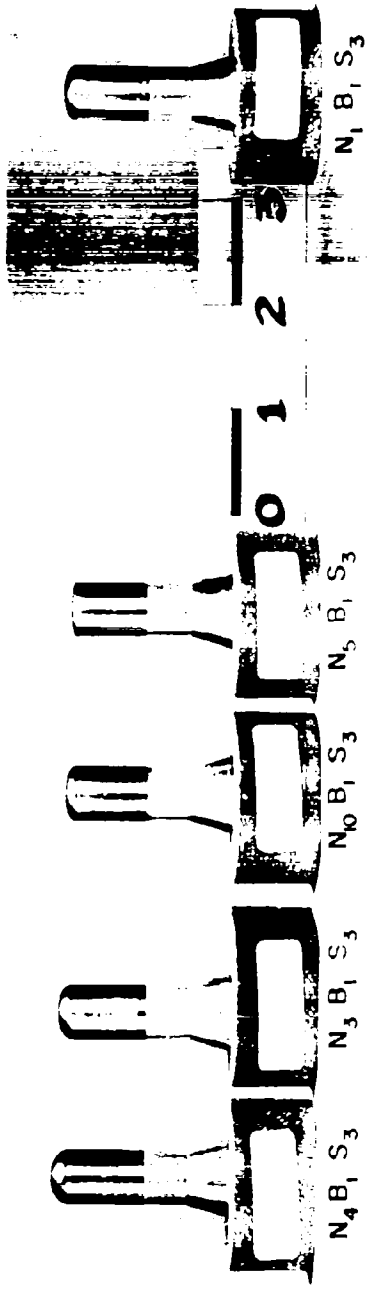

FIG. 2 THE 0.5 INCH BODY DIAMETER MODEL

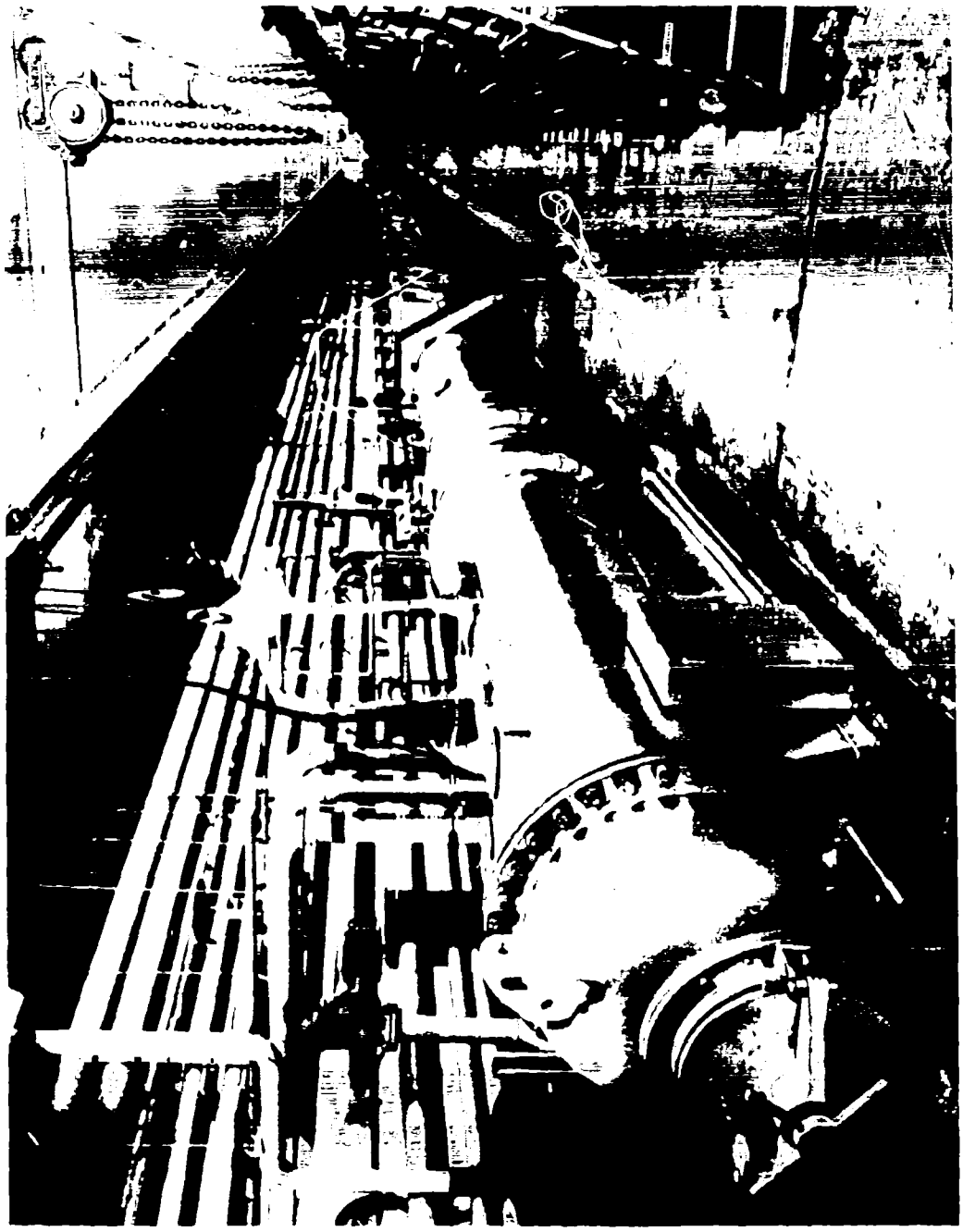

FIG. 3 NOL PRESSURIZED BALLISTICS RANGE

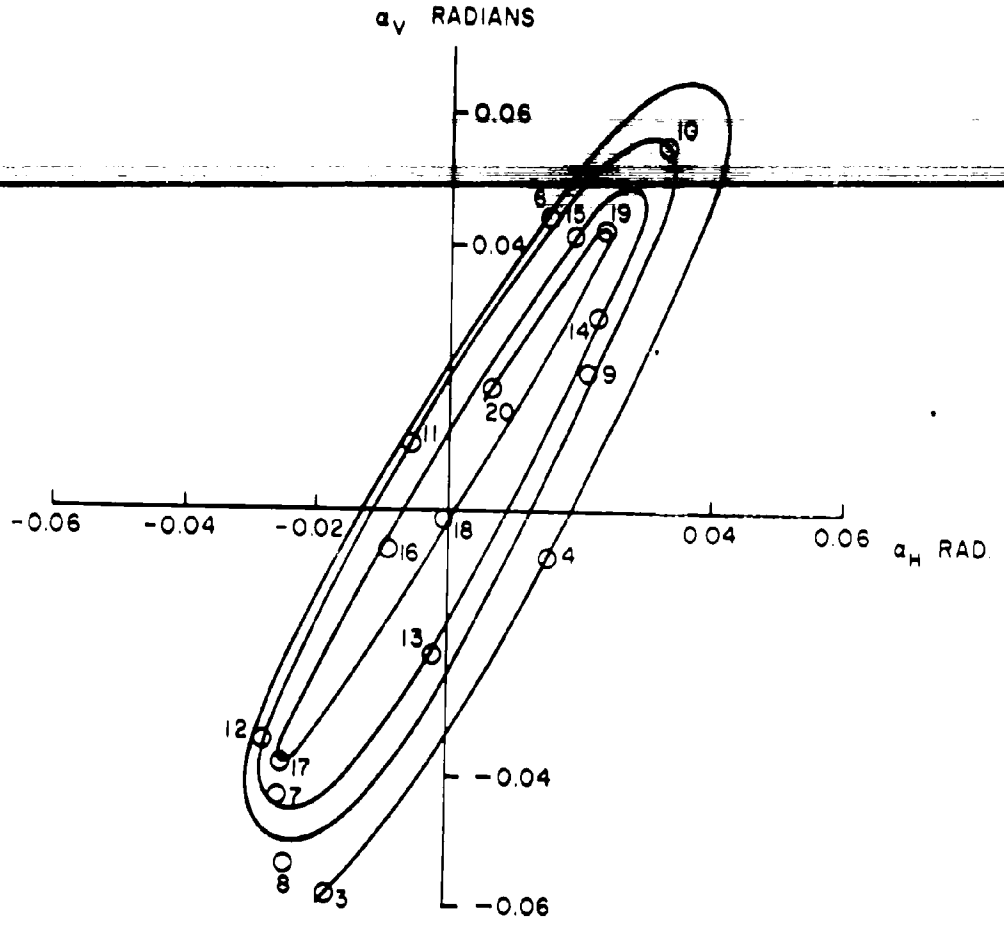

FIG. 4A YAWING MOTION OF MODELS

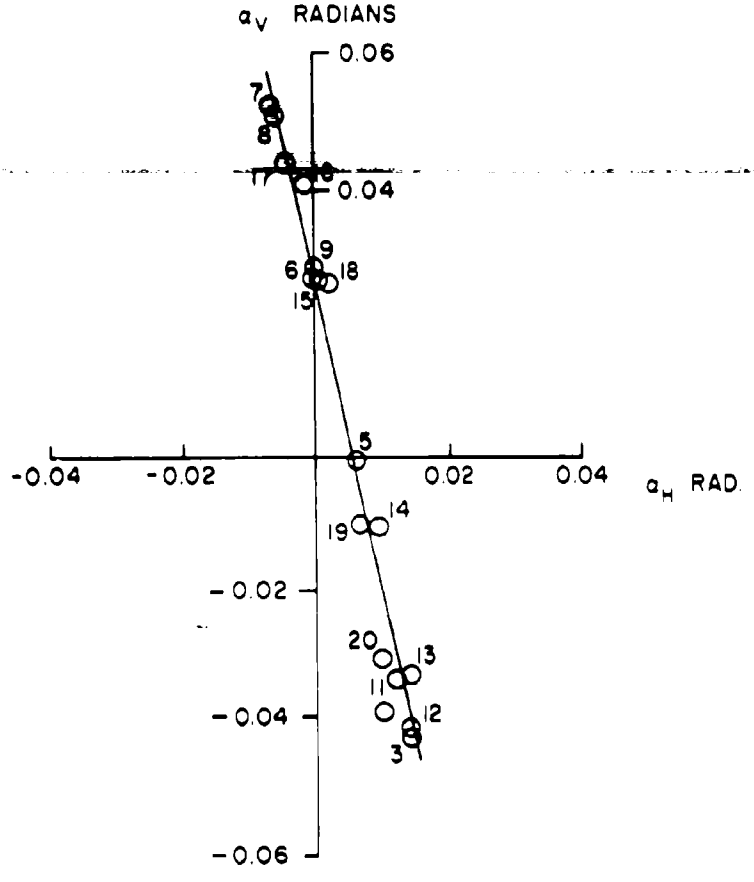

FIG. 4B YAWING MOTION OF MODELS

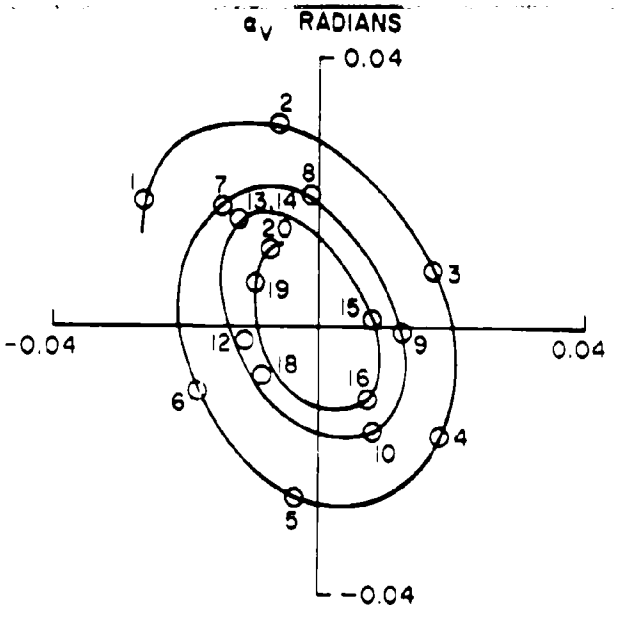

FIG. 4C YAWING MOTION OF MODELS

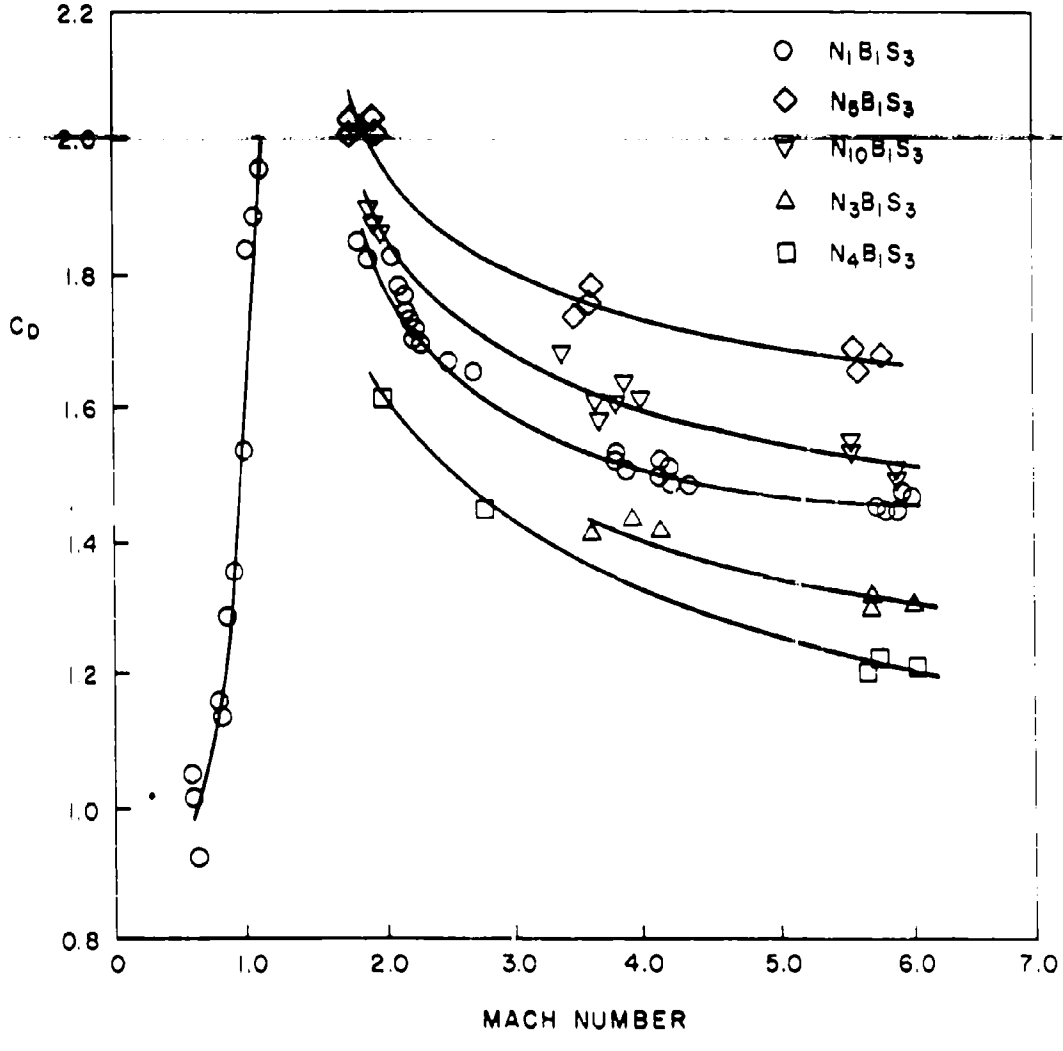

FIG. 5 C_D VERSUS MACH NUMBER

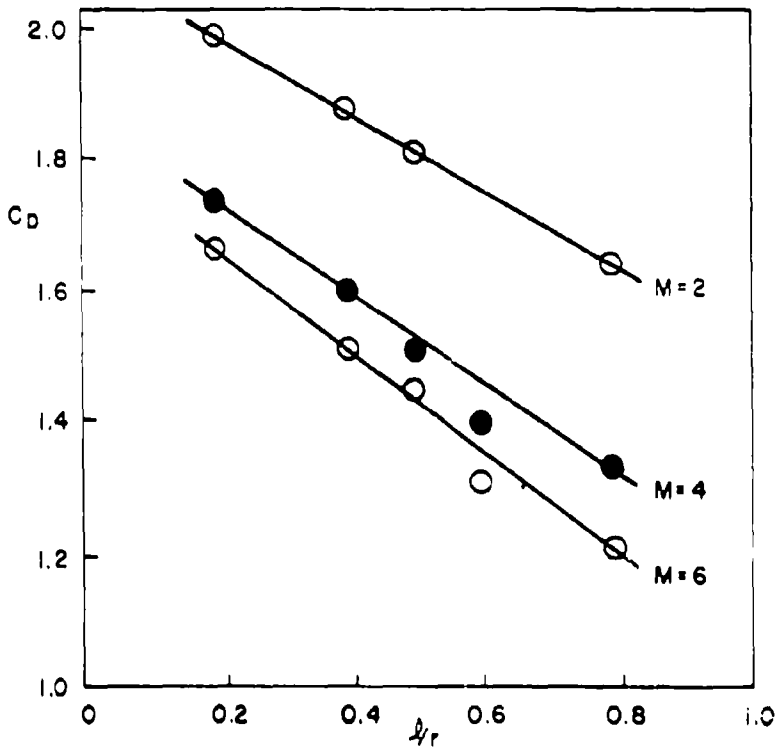

FIG.6 C_D VERSUS NOSE BLUNTNESS RATIO ℓ/r

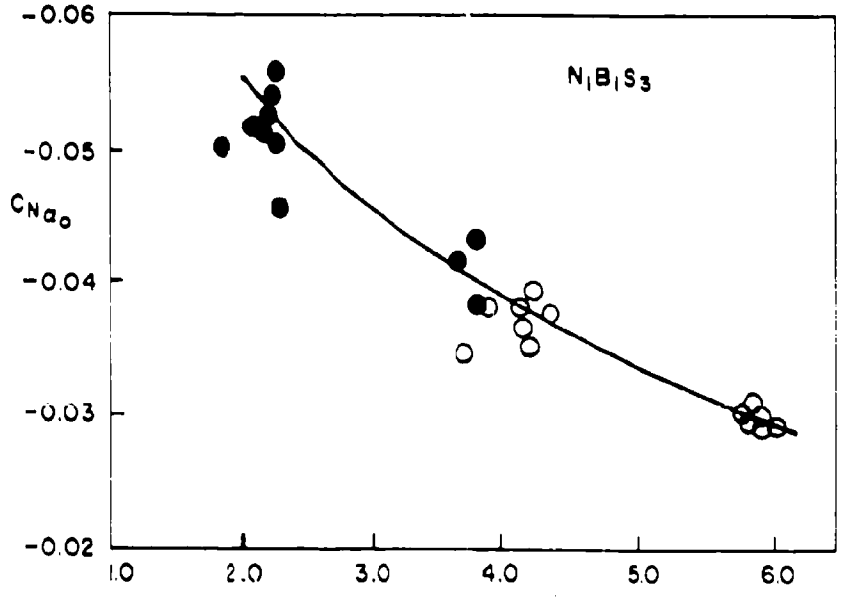

SOLID POINTS NOT CORRECTED TO ZERO YAW

FIG. 7A $C_{N\alpha_o}$ VERSUS MACH NUMBER

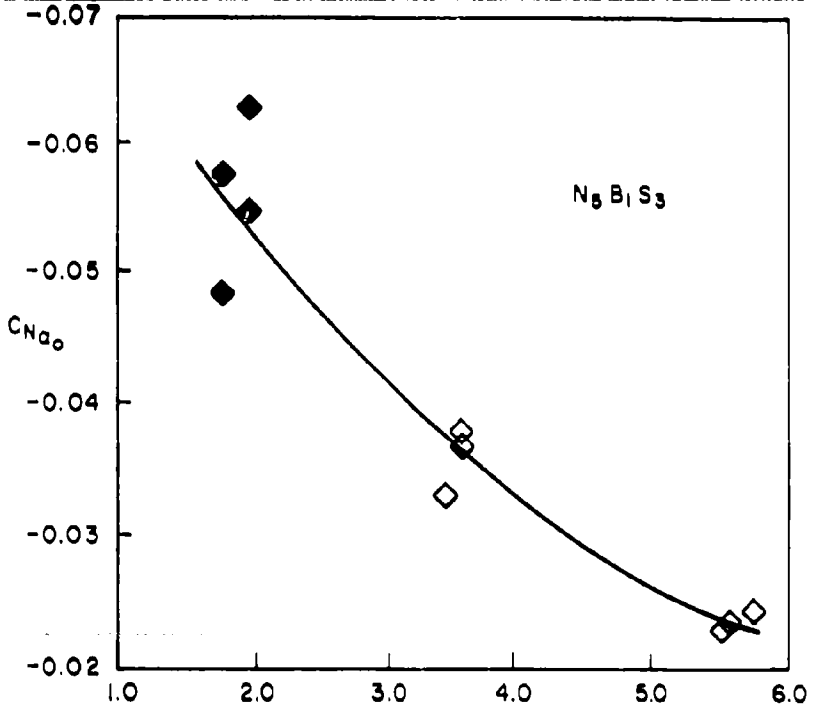

SOLID POINTS NOT CORRECTED TO ZERO YAW

FIG. 7B $C_{N_{\alpha_o}}$ VERSUS MACH NUMBER

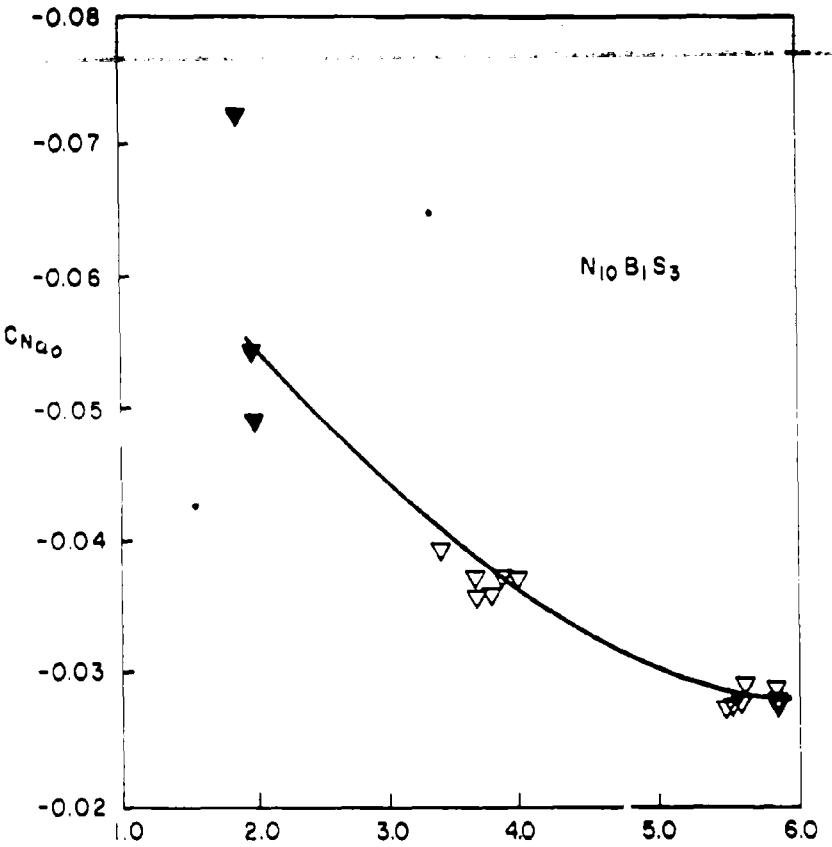

SOLID POINTS NOT CORRECTED TO ZERO YAW

FIG. 7C $C_{N_{\alpha_0}}$ VERSUS MACH NUMBER

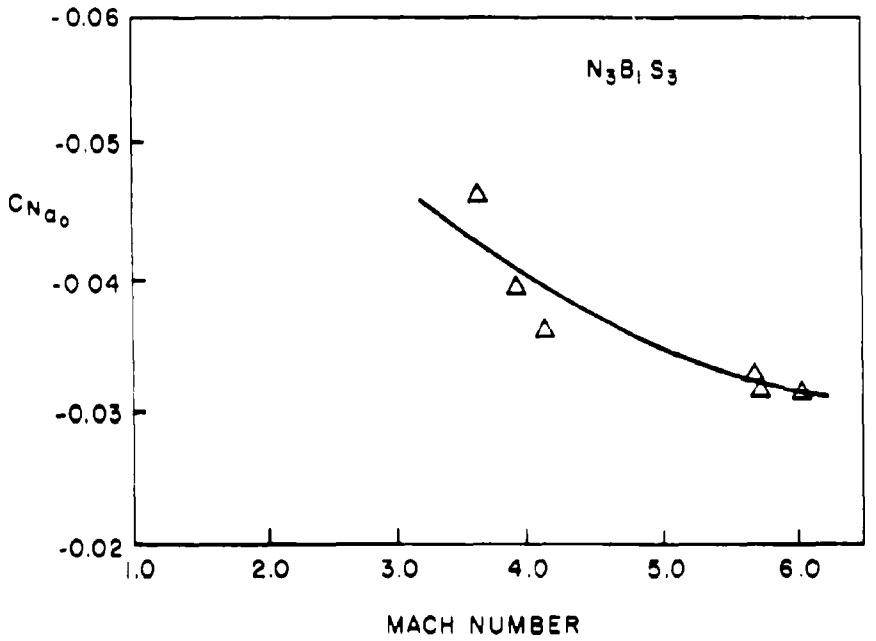

FIG. 7D $C_{N\alpha_o}$ VERSUS MACH NUMBER

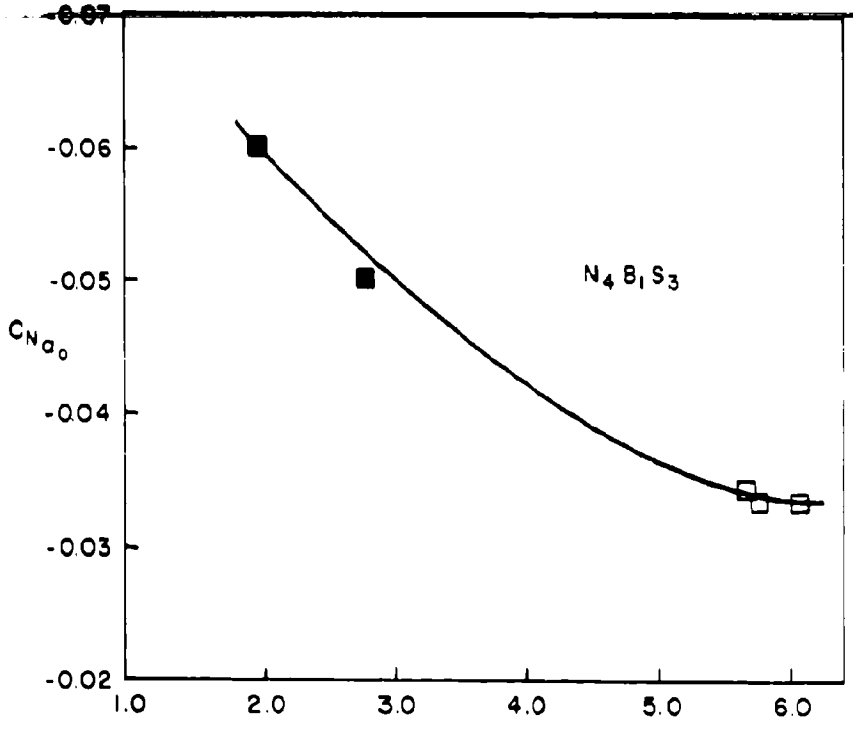

SOLID POINTS NOT CORRECTED TO ZERO YAW

FIG. 7E $C_{N\alpha_0}$ VERSUS MACH NUMBER

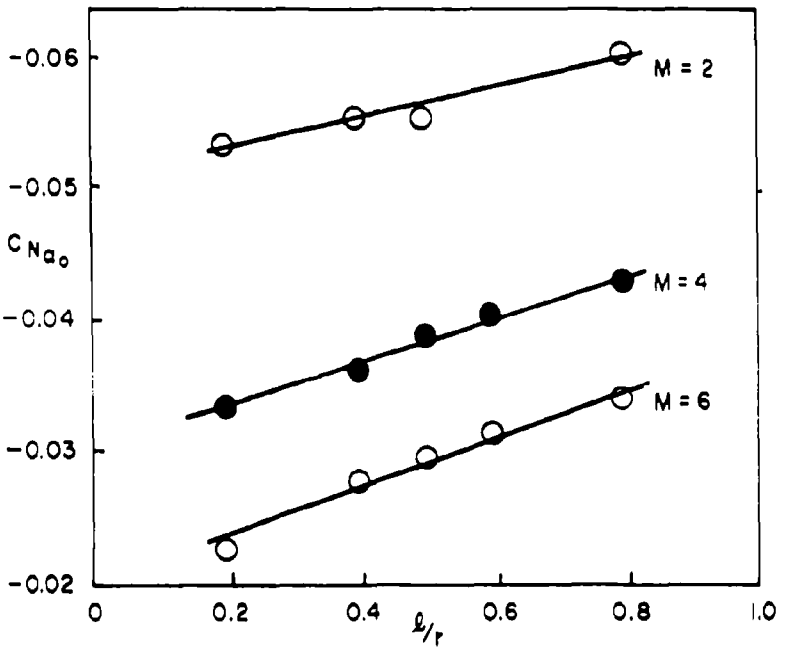

FIG.8 $C_{N_{\alpha_o}}$ VERSUS NOSE BLUNTNESS RATIO ℓ/r

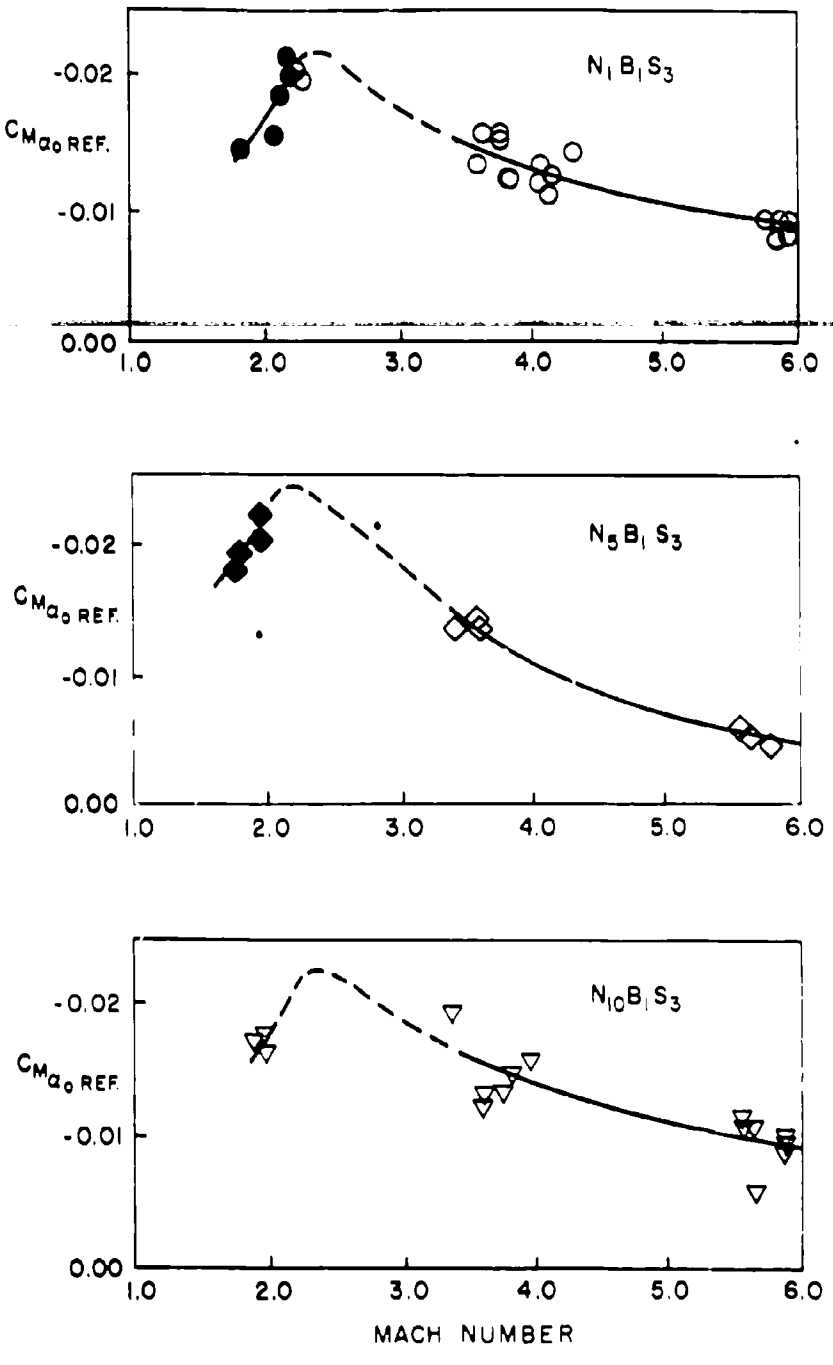

SOLID POINTS NOT CORRECTED TO ZERO YAW

FIG. 9A $C_{M_{\alpha_0 REF.}}$ VERSUS MACH NUMBER

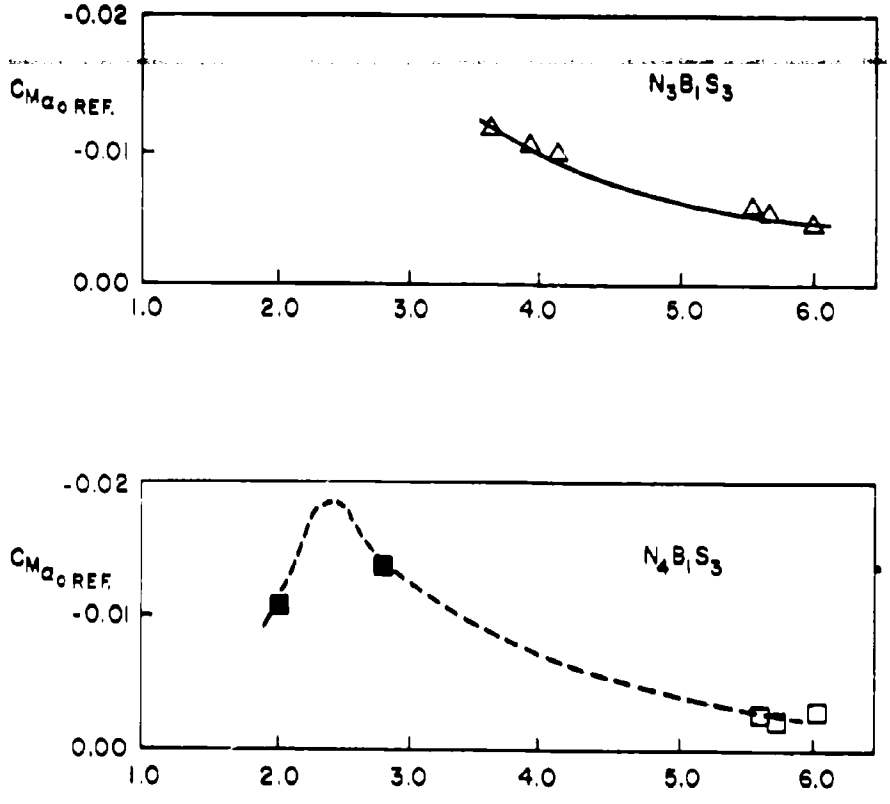

MACH NUMBER
SOLID POINTS NOT CORRECTED TO ZERO YAW
FIG. 9B $C_{M\alpha_{o\ REF.}}$ VERSUS MACH NUMBER

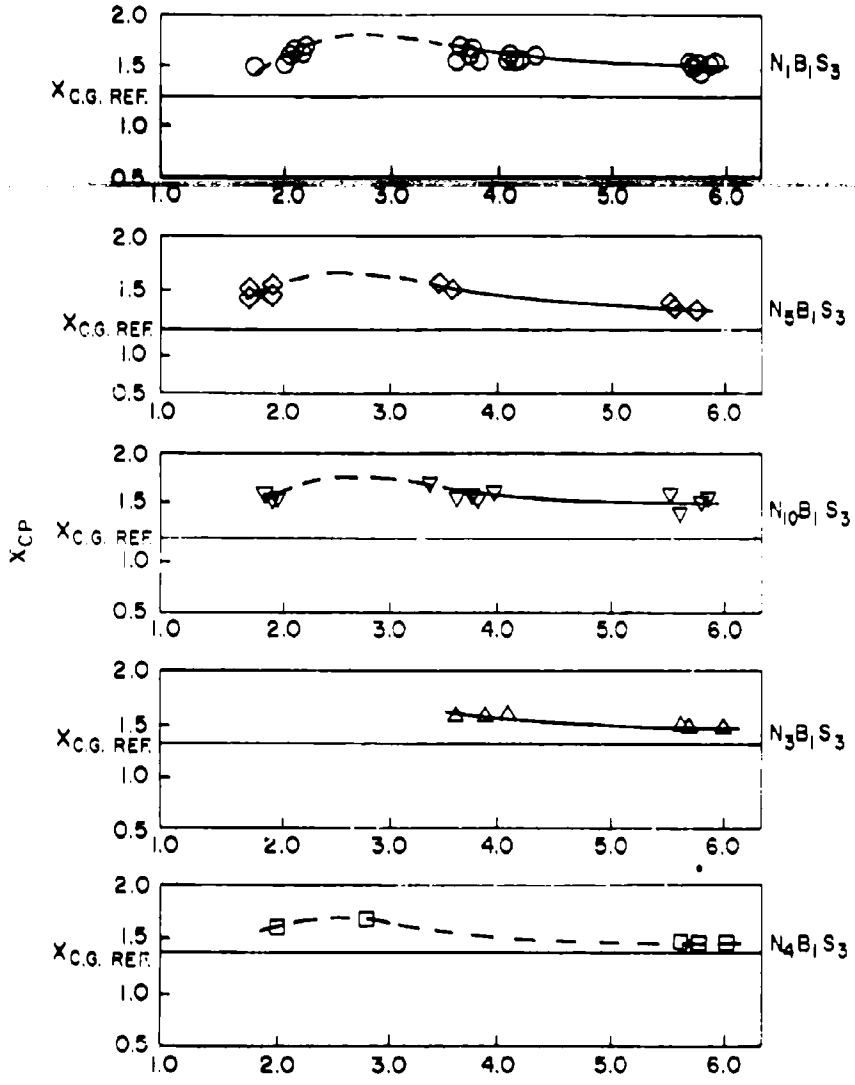

FIG. 10 $X_{C.P.}$ VERSUS MACH NUMBER
$X_{C.P.}$ AND $X_{C.G.\ REF.}$ IN CALIBERS FROM TIP OF NOSE

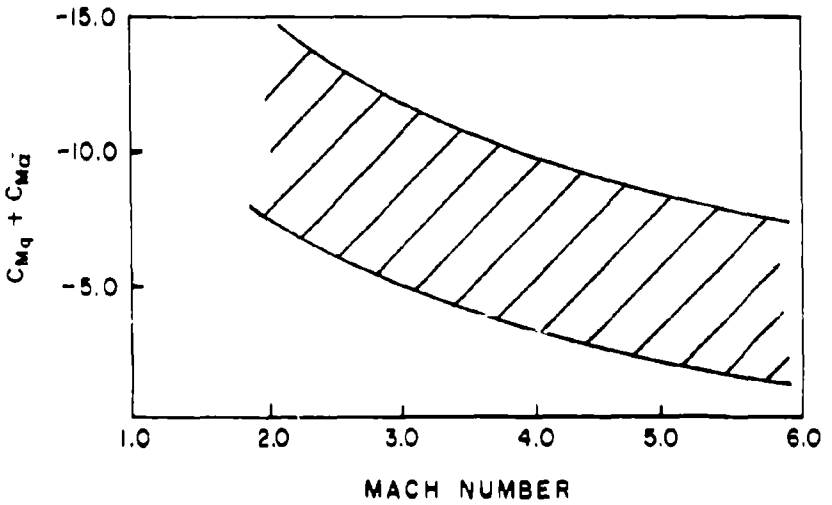

FIG. 11 $C_{Mq} + C_{M\dot{\alpha}}$ VERSUS MACH NUMBER

Naval Ordnance Laboratory, White Oak, Md.
(NOL technical report 61-35)
BALLISTICS RANGE FIRINGS FOR DETERMINATION OF DRAG AND STABILITY OF MODELS OF FIVE POLARIS CONFIGURATIONS (U), by Zigurds J. Levensteins. 11 Aug. 1961. 6p., illus., charts, tables, diagrs. (Ballistics research report 42). Task NOL-335.
CONFIDENTIAL

Drag and stability characteristics of models of five Polaris re-entry body configurations were determined. Variable parameter for configurations was the bluntness of the nose. Investigation was conducted at Mach numbers between two and six. Boundary layer flow over surface of models was turbulent. It was found that slope of normal force coefficient is smaller the blunter the nose of model. A maximum in static stability of models was observed between Mach numbers two and three. Dynamic stability coefficients were found to be stabilizing.

1. Missiles - Polaris
2. Missiles - Re-entry
3. Missiles - Drag
4. Missiles - Stability
I. Title
II. Levensteins, Zigurds J.
III. Series
IV. Project

Abstract card is confidential

DOWNGRADED AT 3 YEAR INTERVALS: DECLASSIFIED AFTER 12 YEARS. DOD DIR 5200.10.

Naval Ordnance Laboratory, White Oak, Md.
(NOL technical report 61-35)
BALLISTICS RANGE FIRINGS FOR DETERMINATION OF DRAG AND STABILITY OF MODELS OF FIVE POLARIS CONFIGURATIONS (U), by Zigurds J. Levensteins. 11 Aug. 1961. 6p., illus., charts, tables, diagrs. (Ballistics research report 42). Task NOL-335.
CONFIDENTIAL

Drag and stability characteristics of models of five Polaris re-entry body configurations were determined. Variable parameter for configurations was the bluntness of the nose. Investigation was conducted at Mach numbers between two and six. Boundary layer flow over surface of models was turbulent. It was found that slope of normal force coefficient is smaller the blunter the nose of model. A maximum in static stability of models was observed between Mach numbers two and three. Dynamic stability coefficients were found to be stabilizing.

1. Missiles - Polaris
2. Missiles - Re-entry
3. Missiles - Drag
4. Missiles - Stability
I. Title
II. Levensteins, Zigurds J.
III. Series
IV. Project

Abstract card is confidential

DOWNGRADED AT 3 YEAR INTERVALS: DECLASSIFIED AFTER 12 YEARS. DOD DIR 5200.10.

Naval Ordnance Laboratory, White Oak, Md.
(NOL technical report 61-35)
BALLISTICS RANGE FIRINGS FOR DETERMINATION OF DRAG AND STABILITY OF MODELS OF FIVE POLARIS CONFIGURATIONS (U), by Zigurds J. Levensteins. 11 Aug. 1961. 6p., illus., charts, tables, diagrs. (Ballistics research report 42). Task NOL-335.
CONFIDENTIAL

Drag and stability characteristics of models of five Polaris re-entry body configurations were determined. Variable parameter for configurations was the bluntness of the nose. Investigation was conducted at Mach numbers between two and six. Boundary layer flow over surface of models was turbulent. It was found that slope of normal force coefficient is smaller the blunter the nose of model. A maximum in static stability of models was observed between Mach numbers two and three. Dynamic stability coefficients were found to be stabilizing.

1. Missiles - Polaris
2. Missiles - Re-entry
3. Missiles - Drag
4. Missiles - Stability
I. Title
II. Levensteins, Zigurds J.
III. Series
IV. Project

Abstract card is confidential

DOWNGRADED AT 3 YEAR INTERVALS: DECLASSIFIED AFTER 12 YEARS. DOD DIR 5200.10.

Naval Ordnance Laboratory, White Oak, Md.
(NOL technical report 61-35)
BALLISTICS RANGE FIRINGS FOR DETERMINATION OF DRAG AND STABILITY OF MODELS OF FIVE POLARIS CONFIGURATIONS (U), by Zigurds J. Levensteins. 11 Aug. 1961. 6p., illus., charts, tables, diagrs. (Ballistics research report 42). Task NOL-335.
CONFIDENTIAL

Drag and stability characteristics of models of five Polaris re-entry body configurations were determined. Variable parameter for configurations was the bluntness of the nose. Investigation was conducted at Mach numbers between two and six. Boundary layer flow over surface of models was turbulent. It was found that slope of normal force coefficient is smaller the blunter the nose of model. A maximum in static stability of models was observed between Mach numbers two and three. Dynamic stability coefficients were found to be stabilizing.

1. Missiles - Polaris
2. Missiles - Re-entry
3. Missiles - Drag
4. Missiles - Stability
I. Title
II. Levensteins, Zigurds J.
III. Series
IV. Project

Abstract card is confidential

DOWNGRADED AT 3 YEAR INTERVALS: DECLASSIFIED AFTER 12 YEARS. DOD DIR 5200.10.

External Distribution List

No. of Copies	
	Director, Special Projects Department of the Navy Washington 25, D. C.
2	Attn: SP-272
	Commander, U. S. Naval Ordnance Test Station China Lake, California
1	Attn: Technical Library
	Director, Aberdeen Proving Ground Aberdeen, Maryland
1	Attn: Technical Information Branch
1	Attn: Ballistics Research Laboratory
	ASTIA Document Service Center Arlington Hall Station
10	Arlington 12, Virginia
	Commander, AEDC Tullahoma, Tennessee
1	Attn: Technical Library
	NASA Ames Research Center Moffett Field, California
1	Attn: Librarian
	NASA Langley Research Center Langley Field Hampton, Virginia
1	Attn: Librarian
	NASA 1512 H Street, N.W.
1	Washington 25, D. C.
	Bureau of Naval Weapons Representative (Special Projects Office) P. O. Box 504 Sunnyvale, California
1	Attn: SpL-314
	Lockheed Missiles and Space Division P. O. Box 504 Sunnyvale, California
1	Attn: Mr. A. W. Meijer
1	Attn: Mrs. J. Vaughn
1	Attn: Mr. J. Howes